

## Host-Guest Synergistic Regulation of Multi-Step Spin-Crossover Behavior in a Hofmann-Type Complex

Kai-Ping Xie,<sup>\*a</sup> Xiao-Yin Weng,<sup>a</sup> Kai-Ye Lin,<sup>a</sup> Jing-Yin Liu,<sup>a</sup> Ming Lu,<sup>a</sup> Zi-Yi Du,<sup>d</sup> Zhong-Li Peng,<sup>a</sup> Yi-Fei Deng,<sup>\*c</sup> Si-Guo Wu,<sup>\*b</sup> and Guo-Cong Liu<sup>\*a</sup>

<sup>a</sup> School of Chemistry and Materials Engineering, Huizhou University, Huizhou, 516007, P. R. China, E-mail: [xiekp@hzu.edu.cn](mailto:xiekp@hzu.edu.cn); [gcl\\_109@hzu.edu.cn](mailto:gcl_109@hzu.edu.cn)

<sup>b</sup> Key Laboratory of Bioinorganic and Synthetic Chemistry of Ministry of Education, School of Chemistry, IGCME, GBRCE for Functional Molecular Engineering, Sun Yat-Sen University, Guangzhou 510275, P. R. China, E-mail: [wusg6@mail.sysu.edu.cn](mailto:wusg6@mail.sysu.edu.cn)

<sup>c</sup> Department of Chemistry, Southern University of Science and Technology, Shenzhen 518055, P. R. China, E-mail: [dengyf@sustech.edu.cn](mailto:dengyf@sustech.edu.cn)

<sup>d</sup> School of Environmental and Chemical Engineering, Foshan University, Foshan 528000, China

---

## Table of Contents

Powder X-ray diffraction.....	1
IR spectrum.....	1
Thermogravimetric analysis.....	2
Magnetic susceptibility.....	2
DSC measurements.....	3
1 <sup>st</sup> differential curve of magnetic data.....	4
Temperature dependence of the relaxation times.....	4
Photomagnetic properties.....	5
Asymmetric unit.....	6
Overlapped structures.....	7

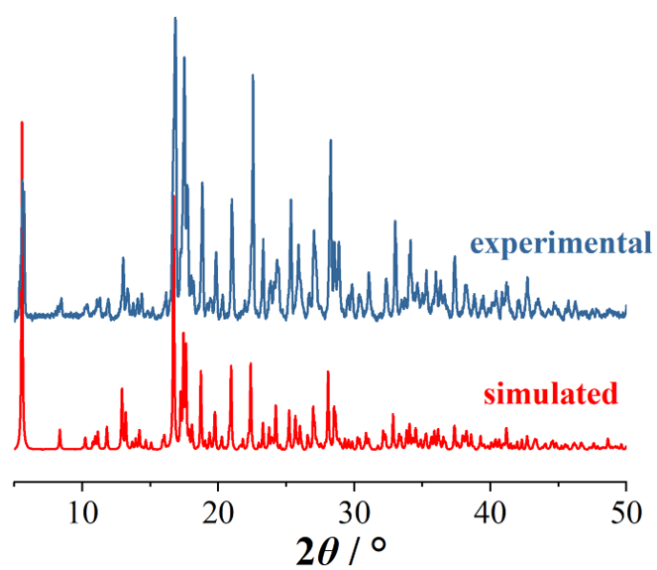


**Figure S1.** Powder X-ray diffraction data of **1**.

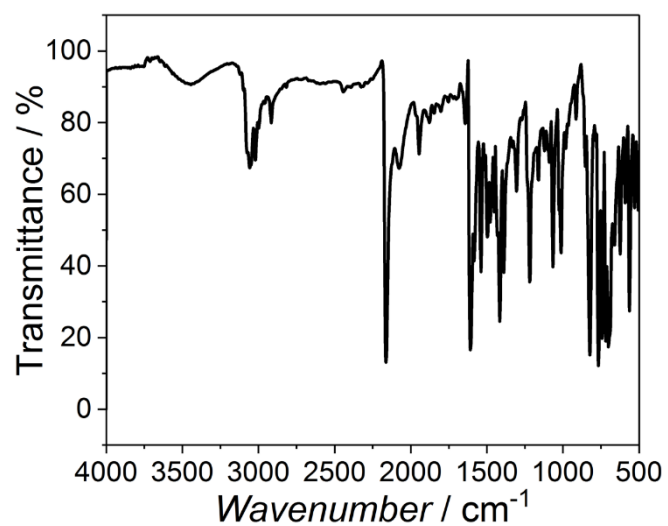


**Figure S2.** IR spectrum of **1**. FT-IR spectra were acquired on a Thermo Nicolet AVATAR 330 spectrometer (room temperature; solid-state KBr pellets; 4000–40  $\text{cm}^{-1}$ ).

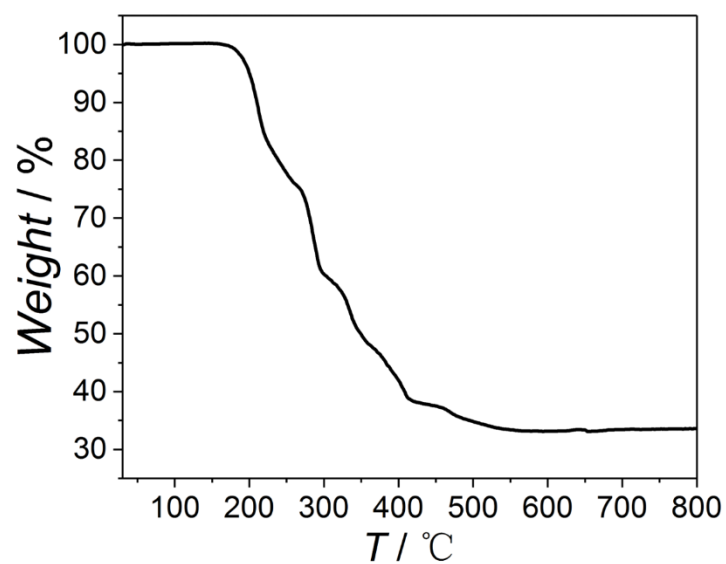


**Figure S3.** Thermogravimetric analysis of **1**.

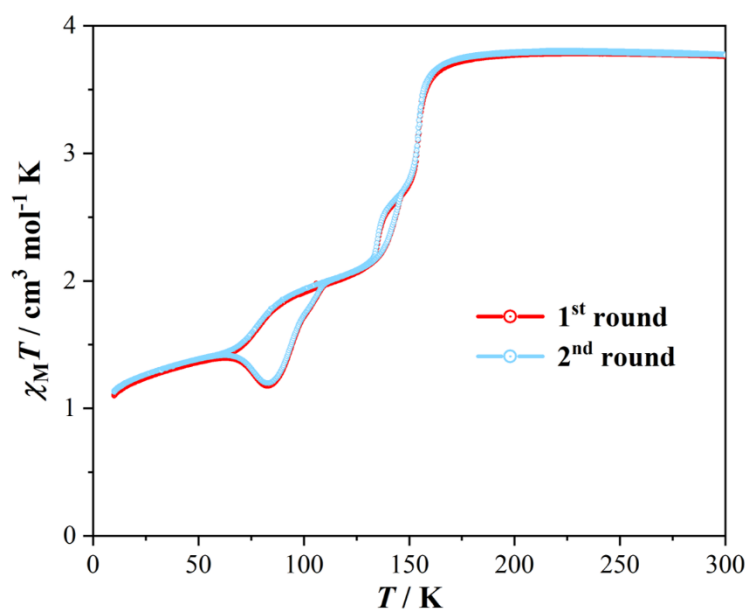


**Figure S4.** Two consecutive cycles of variable-temperature magnetic susceptibility data for **1** at 2 K/min.

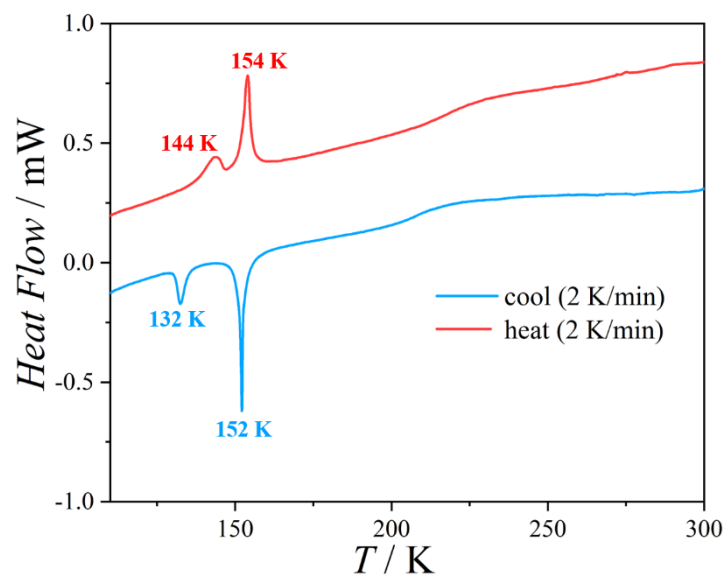


**Figure S5.** Differential scanning calorimetry (DSC) measurements of **1** at 2 K min<sup>-1</sup>.

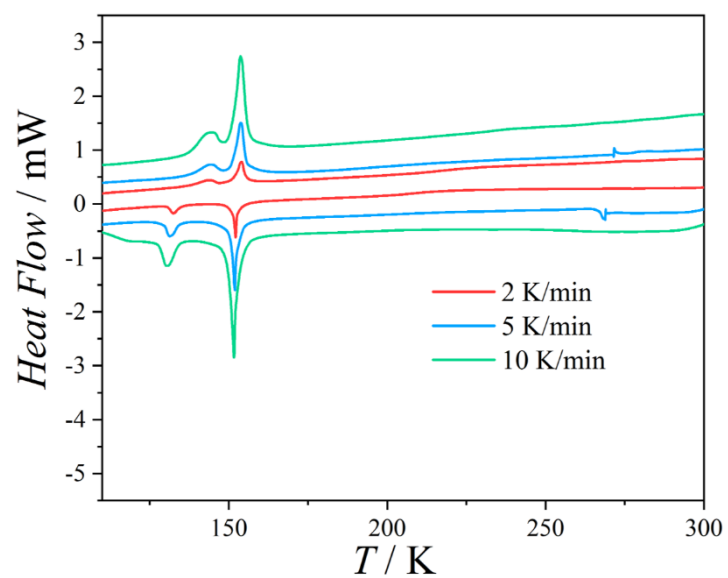


**Figure S6.** DSC measurements were performed at different scan rates of 2, 5 and 10 K/min.

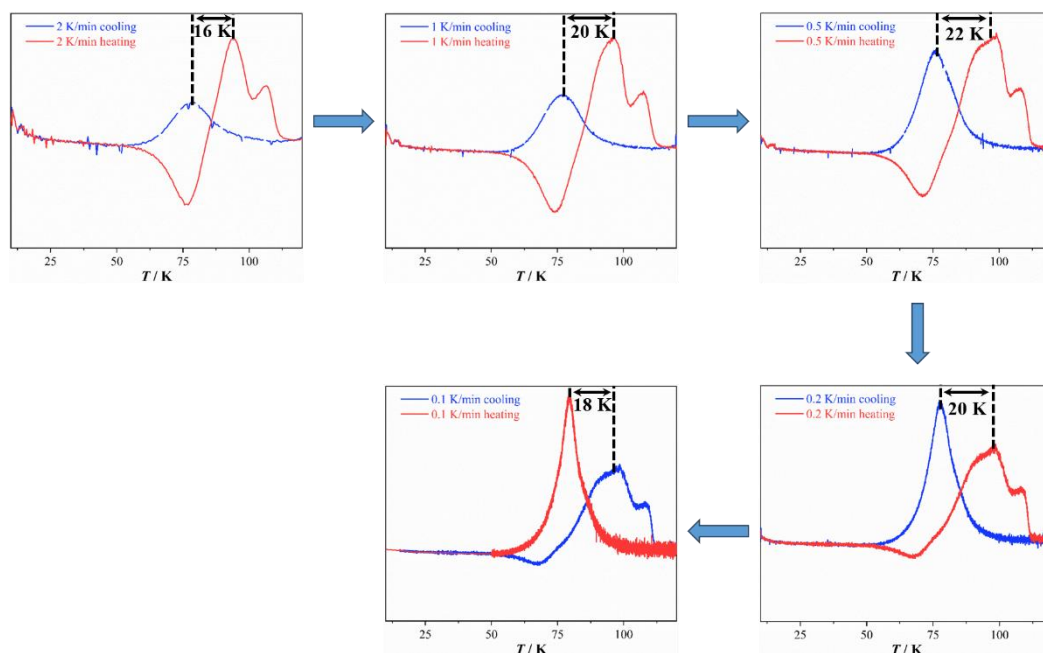


**Figure S7.** 1<sup>st</sup> differential curve of magnetic data in the low-temperature region under different scan rates for **1**.

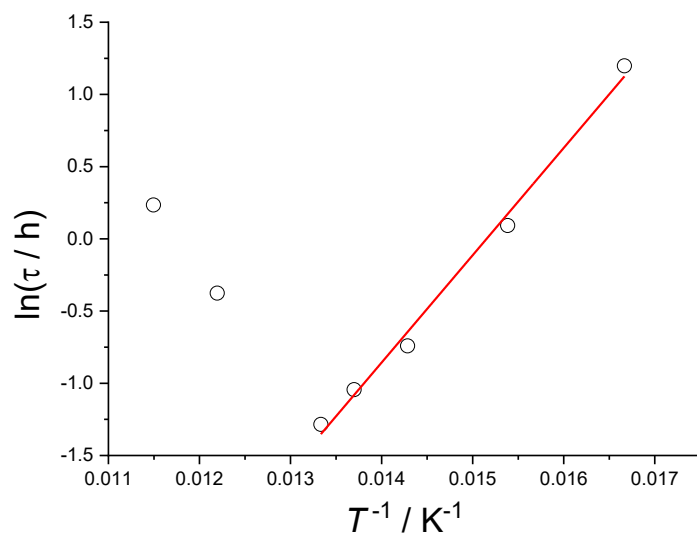


**Figure S8.** Temperature dependence of the relaxation times. Solid line represents the fit to the data.

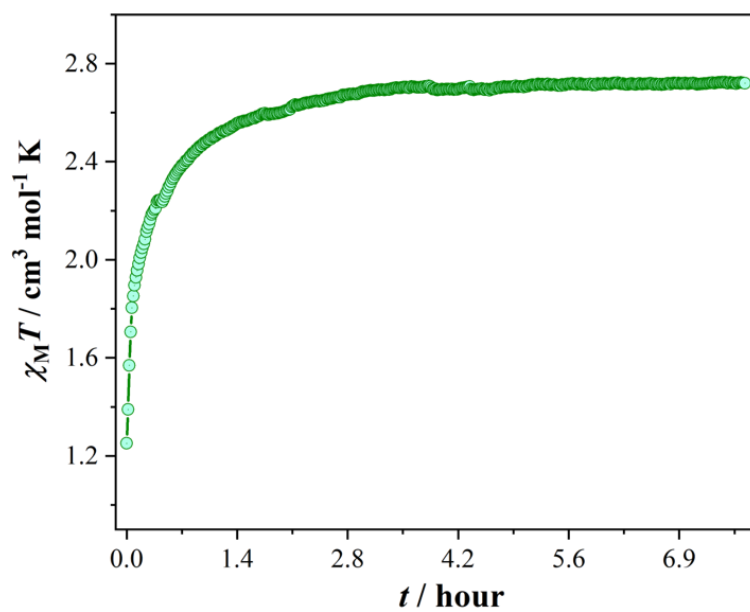


**Figure S9.** Molar magnetic susceptibility  $\chi_M T$  versus time for **1** during LIESST under 532 nm light irradiation at 10 K.

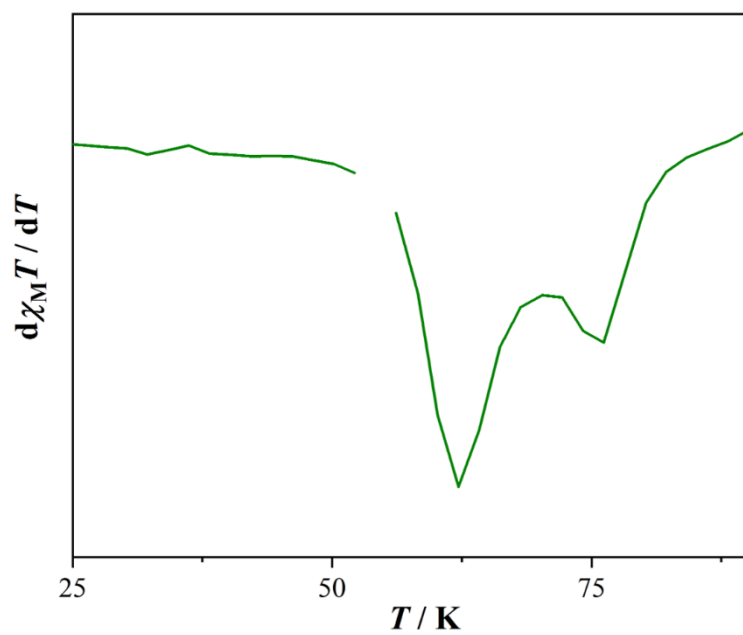


**Figure S10.** 1<sup>st</sup> derivative of the photomagnetic data of **1** under 532 nm light irradiation.

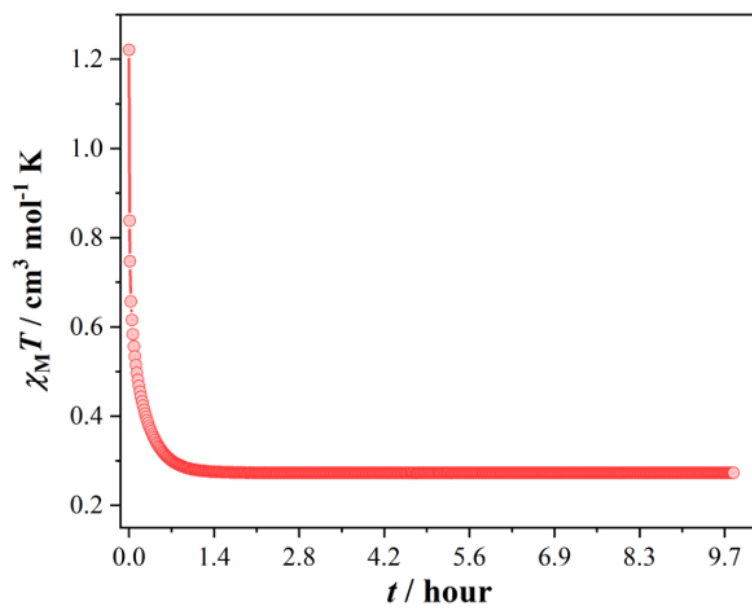


**Figure S11.** Molar magnetic susceptibility  $\chi_M T$  versus time for **1** during reverse-LIESST under 808 nm light irradiation at 10 K.

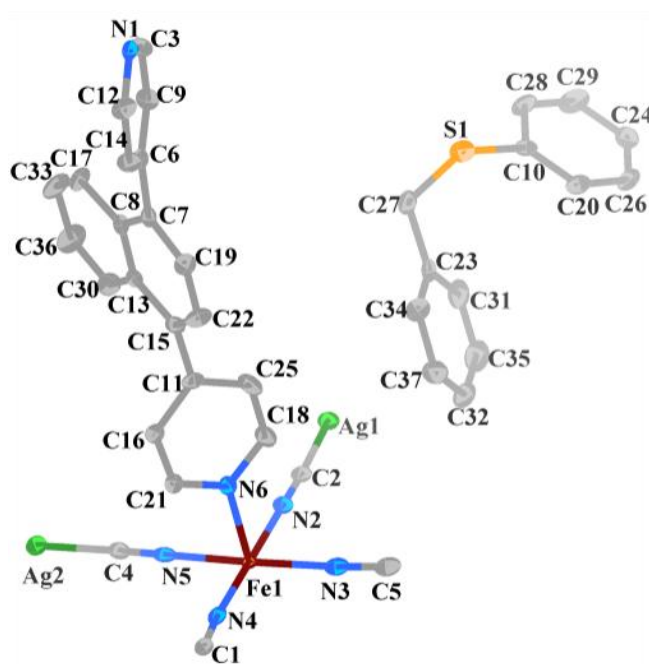


**Figure S12.** Asymmetric unit of **1**. Hydrogen atoms are omitted for clarity.

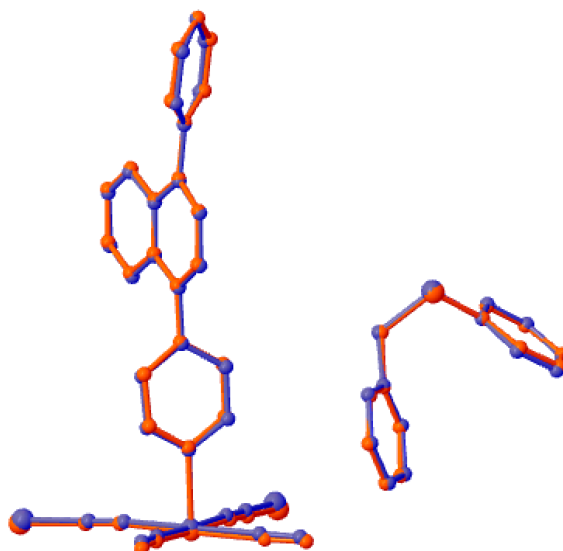


**Figure S13.** Overlapped structures of **1** at 300 K (red) and 80 K (blue).

**Table S1.** Crystallographic data and structural refinements for **1** at different temperatures.

Formula	C <sub>37</sub> H <sub>26</sub> Ag <sub>2</sub> FeN <sub>6</sub> S				
<i>Mr</i>	858.29				
<i>T</i> / K	80(2)	120(2)	150(2)	180(2)	300(2)
Crystal system	monoclinic				
Space group	<i>P</i> 2 <sub>1</sub> / <i>c</i>				
<i>a</i> /Å	15.6148(8)	15.6754(12)	15.7621(14)	15.8525(13)	15.891(6)
<i>b</i> /Å	10.4036(6)	10.4498(7)	10.5278(9)	10.5979(8)	10.605(5)
<i>c</i> /Å	20.7290(11)	20.8485(14)	20.9806(16)	21.1073(14)	21.199(9)
$\beta$ /°	91.933(2)	92.335(3)	92.742(3)	93.065(3)	92.244(17)
<i>V</i> /Å <sup>3</sup>	3365.5(3)	3412.2(4)	3477.5(5)	3541.0(5)	3570(3)
<i>Z</i>	4				
$\rho_{\text{calc}}/\text{cm}^3$	1.694	1.671	1.639	1.610	1.597
<i>R</i> <sub>int</sub>	0.0794	0.0980	0.1313	0.1102	0.0348
<i>R</i> <sub>1</sub> ( <i>I</i> > 2σ( <i>I</i> )) <sup>a</sup>	0.0392	0.0423	0.0557	0.0539	0.0414
<i>wR</i> <sub>2</sub> (all data)	0.0826	0.0891	0.1267	0.1169	0.0963
GOF on <i>F</i> <sup>2</sup>	1.095	1.048	1.044	1.051	1.137
largest diff. peak/hole	1.64/-0.57	1.47/-0.56	1.42/-0.85	1.68/-0.82	0.70/-0.68

$$^a R_1 = \sum ||F_o| - |F_c|| / \sum |F_o|. \quad wR_2 = [\sum w(F_o^2 - F_c^2)^2 / \sum w(F_o^2)^2]^{1/2}$$

**Table S2.** Edge-to-face  $\pi \cdots \pi$  interactions between pyridine rings of bpn ligands and guest benzene rings in **1**.

Parameter	80 K	120 K	150 K	180 K	300 K
<i>d</i> <sub>1</sub> <sup>[a]</sup>	4.058(2)	4.072(2)	4.096(3)	4.129(2)	4.153(2)
<i>l</i> <sup>[b]</sup>	3.241(2)	3.241(2)	3.251(2)	3.282(2)	3.318(1)
$\theta$ <sup>[c]</sup>	24.31(2)	23.31(1)	22.39(2)	21.80(2)	20.75(2)

<sup>a</sup>The edge-to-face  $\pi \cdots \pi$  interaction between the phenyl moiety of guest and pyridyl groups of bpn ligands (Å);

<sup>b</sup>The shortest distance of H-to-ring center (Å); <sup>c</sup>The angle between phenyl moiety of guest and pyridyl groups of bpn ligands (°).

**Table S3.** Selected bond lengths and angles around the iron center at different temperatures.

Parameter		80 K	120 K	150 K	180 K	300 K
Fe-N bond length / Å	Fe-N1	2.101(3)	2.137(3)	2.180(3)	2.225(3)	2.239(3)
	Fe-N2	2.011(3)	2.047(3)	2.087(5)	2.133(4)	2.142(3)
	Fe-N3	2.016(3)	2.043(3)	2.095(4)	2.142(4)	2.148(3)
	Fe-N4	2.009(3)	2.033(3)	2.068(5)	2.120(4)	2.121(3)
	Fe-N5	2.018(3)	2.052(3)	2.118(4)	2.161(4)	2.168(3)
	Fe-N6	2.081(3)	2.124(3)	2.178(5)	2.240(3)	2.255(3)
N-Fe-N angle / °	N1-Fe-N2	91.85(1)	92.13(1)	92.27(2)	92.55(1)	92.45(1)
	N1-Fe-N3	91.80(1)	92.14(1)	93.09(2)	93.49(1)	93.01(1)
	N1-Fe-N4	90.63(1)	90.30(1)	90.25(1)	90.22(1)	90.01(1)
	N1-Fe-N5	87.37(1)	87.42(1)	86.64(2)	86.52(1)	87.25(1)
	N6-Fe-N2	90.83(1)	91.04(1)	90.83(2)	90.73(1)	91.45(1)
	N6-Fe-N3	91.38(1)	91.68(1)	91.56(2)	91.88(1)	92.36(1)
	N6-Fe-N4	86.77(1)	86.65(1)	86.81(1)	86.72(1)	86.28(1)
	N6-Fe-N5	89.63(1)	88.98(1)	88.96(2)	88.36(1)	87.70(1)
	N2-Fe-N3	88.17(1)	88.01(1)	87.83(2)	87.49(2)	87.56(1)
	N3-Fe-N4	90.41(1)	90.26(1)	90.18(2)	90.19(2)	90.40(1)
	N4-Fe-N5	93.45(1)	93.73(1)	94.33(2)	94.26(2)	94.25(1)
	N5-Fe-N2	88.00(1)	88.02(1)	87.68(2)	88.07(2)	87.79(1)
Fe-N-C angle / °	Fe-N2-C2	177.07(3)	176.12(3)	174.33(5)	172.69(4)	174.44(3)
	Fe-N3-C5	174.93(3)	173.92(3)	174.15(5)	172.69(4)	174.47(3)
	Fe-N4-C1	174.33(3)	173.54(3)	173.22(5)	171.42(4)	173.09(3)
	Fe-N5-C4	172.96(3)	171.86(3)	171.46(5)	170.05(4)	170.42(3)

**Table S4.** Selected crystallographic parameters for **1** at different temperatures.

Parameter	80 K	120 K	150 K	180 K	300 K
$d_{\text{Ag1}\cdots\text{C32}}^{\text{[a]}}$	3.343(4)	3.347(4)	3.375(9)	3.386(7)	3.508(1)
$d_1^{\text{[b]}}$	4.058(2)	4.072(2)	4.096(3)	4.129(2)	4.153(2)
$d_2^{\text{[c]}}$	3.675(5)	3.668(5)	3.676(8)	3.673(8)	3.701(8)
$d_3^{\text{[d]}}$	5.741(6)	5.757(6)	5.765(9)	5.796(9)	5.830(9)
$d_4^{\text{[e]}}$	3.547(4)	3.576(5)	3.633(7)	3.644(7)	3.719(8)
angle <sup>[f]</sup>	40.89(2)	42.24(1)	44.03(2)	45.42(2)	46.15(2)

<sup>a</sup>The distance between Ag1 and C32; <sup>b</sup>The edge-to-face  $\pi\cdots\pi$  interaction between the phenyl moiety of guest and pyridyl groups of bpn ligands; <sup>c</sup> The distance between C20 and C8; <sup>d</sup> The distance between C10 and C36; <sup>e</sup> The distance between C28 and S1; <sup>f</sup>The dihedral angle between benzene.

**Table S5.** Dihedral angles (°) among the three planes of the bpn ligand in **1**—with the naphthalene ring defined as Plane 1 and the two pyridine rings as Planes 2 and 3.

Parameter	80 K	120 K	150 K	180 K	300 K
Plane1-Plane2	45.69(9)	47.28(1)	49.25(2)	50.58(1)	51.61(1)
Plane1-Plane3	80.84(1)	82.15(1)	84.73(1)	86.76(1)	87.74(1)
Plane2-Plane3	54.36(1)	51.53(1)	47.20(2)	44.05(2)	41.74(2)